E-ISSN 2586-9027
Homepage : https://tci-thaijo.org/index.php/SciTechAsia Science & Technology Asia
Vol.30 No.3 July - September 2025 Page: [30-39]
Original research article

Implementing Pressure Sensing Technology for Healthcare Applications

Nyan Lin Mya[1], Jirapath Tharasena[1], Chawanakon Promsila[1], Patt Pootrakul[1], Paweena Kanokhong[1], Somrudee Deepaisarn[1,2,*]

[1] *Sirindhorn International Institute of Technology, Thammasat University, Pathum Thani 12120, Thailand*
[2] *Research Unit in Sustainable Electrochemical Intelligent, Thammasat University, Pathum Thani 12120, Thailand*

Received 16 June 2025; Received in revised form 29 July 2025
Accepted 18 August 2025; Available online 30 September 2025

ABSTRACT

The demand for fitness solutions that are accessible, reasonably priced, and privacy-focused is rising, especially for applications that call for remote monitoring. Yoga is popular, but because of its complexity and range of poses that call for exact posture, it can be difficult to practice remotely. In order to categorize and estimate yoga poses without the need for camera-based monitoring, this project presents a novel pressure-sensing matrix mat (Asana mat) made of Velostat material. The real-time pressure distribution patterns recorded by the Asana mat are analyzed using deep learning models, such as convolutional neural network (CNN) and random forest for pose classification, and hybrid convolutional neural network long short-term memory (CNN-LSTM) architecture for pose estimation. The system is trained on diverse datasets collected from different users, poses, and execution styles to increase robustness. The results demonstrate a high classification accuracy of 98.05% for classifying 10 poses, making the system a non-invasive, user-friendly tool for improving yoga practice even for remote applications. Additionally, for pose estimation, a hybrid CNN-LSTM architecture was created, which achieved a root mean square error of 0.062 for a prediction every 10-sequence length (10 frames). As a result, this privacy-preserving system is advantageous in both therapeutic and home settings. Deep learning models and non-intrusive pressure sensors show promise for a variety of applications, such as personalized fitness coaching, quantitative physical rehabilitation, and healthcare monitoring.

Keywords: Deep learning; Pressure sensing mat; Pose classification; Privacy; Yoga pose classification

***Corresponding author:** somrudee@siit.tu.ac.th **doi:** 10.14456/scitechasia.2025.44

1. Introduction

Exercise and physical activity are essential for preserving and improving health. Exercise reduces the risk of noncommunicable diseases like diabetes, cardiovascular disease, and some types of cancer, improves quality of life, and lowers mortality rates, according to numerous studies [1]. The World Health Organization (WHO) has published that just a little increase in physical activity can have a significant positive influence on the physical, emotional, and social well-being [2, 3].

Yoga, which has its roots in Indian tradition, integrates physical postures, mindfulness, and breath control to promote overall health. Accurate alignment is crucial to avoiding injury, as self-guided practice has grown in popularity during the COVID-19 pandemic. This is leading to an increasing need for easily accessible instruments that support good posture and offer real-time feedback [4].

Recent studies have automatically recognized yoga poses using developments in deep learning and computer vision. Anand Thoutam et al. (2022) developed a deep learning-based system for classifying yoga poses and generating feedback using pose estimation models, such as PoseNet and OpenPose, along with multilayer perceptron (MLP) classifiers. This approach enabled them to achieve a 99.58% classification accuracy. However, this system was trained with only six yoga poses and had trouble recognizing between visually similar poses and occlusion [5]. Saurav et al. (2024) looked into deep learning architectures for real-time yoga pose recognition using hybrid convolutional neural network long short-term memory (CNN-LSTM) and 3D convolutional neural network (3D CNN) models. Their best-performing model achieved 99.65% accuracy and real-time performance at 31 frame per second (FPS) on graphical processing unit (GPU) and 8 FPS on embedded platforms [6]. The models' mean recognition accuracies were 98.80%, 99.07%, 98.19%, and 98.43%. With 82 classes, the Yoga-82 dataset was presented by Verma et al. (2020) as a large-scale benchmark for fine-grained yoga pose classification. However, their own hierarchical variants achieved up to 89.81% Top-1 accuracy at the coarsest level and 79.35% at the finest level, demonstrating the difficulty of fine-grained pose recognition even for advanced models [7]. Their evaluation of state-of-the-art convolutional neural networks revealed that DenseNet-201 achieved a Top-1 accuracy of 74.91% and a Top-5 accuracy of 91.30% on the most difficult (third-level) classification task. Mya et al. (2023), on the other hand, did not discuss yoga pose classification specifically; instead, they concentrated on exercise pose recognition and counting using robust topological landmarks [8].

Therefore, the vision-based systems are still restricted by the subject being blocked, the dependency viewpoint. Moreover, there are privacy concerns, especially in residential or medical settings. These limitations provide research into alternative sensing methods, such as pressure-sensing mats, which can provide pose information without gathering visual data, improving usability and privacy when used.

To address the limitations of image and video-based systems, a pressure-sensing mat was developed using a flexible, low-cost piezoresistive Velostat, which is widely used in posture recognition and healthcare applications [9]. Compared to camera-based systems, pressure-sensing matrix mats offer a privacy advantage because they only record the pressure distribution across a surface, rather than capturing

visual cues that can identify a user or reveal their surroundings. Consequently, because these systems do not gather visual data, they are ideal for sensitive settings such as medical care, rehabilitation, or home monitoring [10, 11].

2. Materials and Methods

2.1 Materials

The system consists of a custom-built Asana mat with a 32×32 pressure sensor array. Asana mat is made of two outer layers with copper tapes placed perpendicular to each other, with a Velostat layer in the middle. as in Fig. 1, an Arduino Mega (Shenzhen, China) for mat data acquisition, and a camera and a computer for video capture. The Arduino reads resistance changes from the mat, mapping them to a 0–1023 range, and transmits the data to a computer. Simultaneously, a camera records participants performing yoga poses, providing synchronized visual data for pose landmark extraction using the MediaPipe Python library [12, 13].

2.2 Data collection

Pressure data from the pressure-sensing mat and pose images from the camera were collected simultaneously. Two datasets were collected. Yoga poses data where participants performed foundational poses, including Boat Pose, Chair Pose, Cobbler's Pose, etc., as shown in Fig. 2, for 10-30 seconds each. These poses are recognized for building strength, flexibility, and balance [12, 13]. Yoga pose data were recorded with multiple repetitions and variations to ensure diversity. Freestyle data, where participants performed various everyday poses and transitions.

Details of participants and collected data are as follow: 4 male and 1 female with age between 22 and 30 years old with

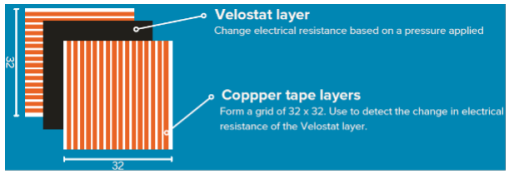

Fig. 1. Asana mat is made of two outer layers with copper tapes placed perpendicular to each other, with a Velostat layer in the middle.

Fig. 2. 10 foundational yoga poses.

normal body mass index (BMI). The data spread is also shown in Fig. 3.

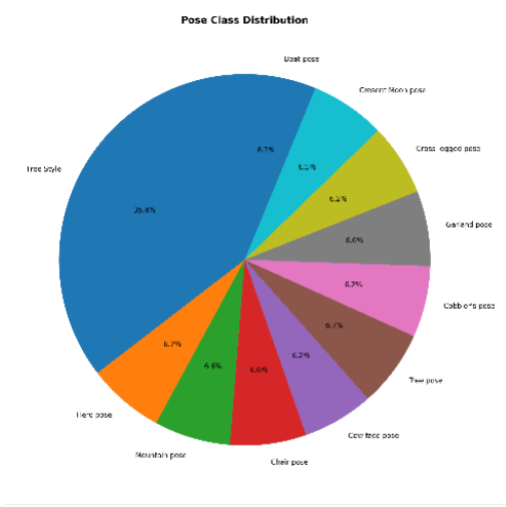

Fig. 3. Class distribution.

2.3 Data preprocessing

Pressure data was calibrated and normalized, and invalid values were removed. Each sample is a 32×32 matrix. Video frames were processed with MediaPipe to

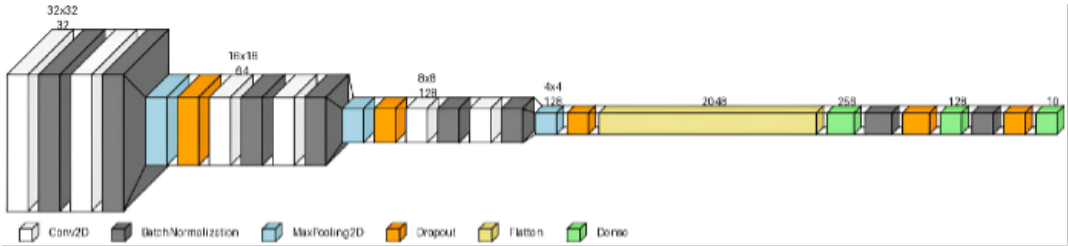

Fig. 4. CNN model architecture used for pressure sensing mat data.

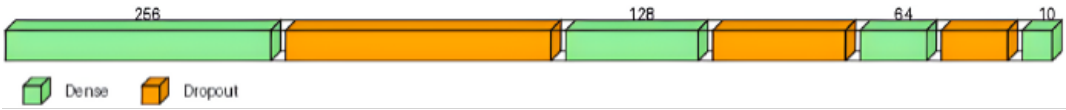

Fig. 5. FCNN model trained with estimated pose data from the camera.

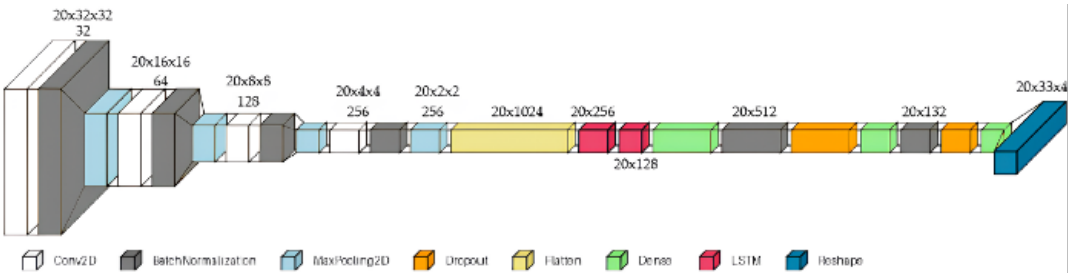

Fig. 6. CNN-LSTM architecture for pose estimation from the mat data.

extract 33 pose landmarks (x, y, z, visibility) [8]. Datasets were synchronized and labeled. For classification, each row includes pressure data, pose landmarks, and pose labels. For pose estimation, sequential datasets were created using a sliding window (sequence lengths: 5, 10, 20, 30). Data augmentation included 90-degree rotations of pressure matrices.

2.4 Model architectures

Three models were used: (1) a convolutional neural network (CNN) Figs. 4 and 12 for classifying yoga poses from pressure data [14]; (2) a fully connected neural network (FCNN) Figs. 5 and 13 for classifying poses from pose landmarks [15]; and (3) a convolutional neural network and long-short term memory (CNN-LSTM) Figs. 6 and 14, for pose estimation, mapping sequences of pressure data to pose landmark sequences [16] (See Figs. 12-14 in the Appendix).

All models were implemented in TensorFlow and evaluated using accuracy, precision, recall, and F1-score for classification, as well as mean square error (MSE) or root mean square error (RMSE) for pose estimation. The pressure dataset has 115,688 samples, split into training (74,040), validation (18,510), and test (23,138) sets. The pose landmark dataset has 28,922 samples, split into training (18,509), validation (4,628), and test (5,785) sets. For pose estimation, the model requires training with both present and past data points. Therefore, the sampling range is varied by sequence length.

For CNN and FCNN models we used Adam as optimizer, sparse categorical cross entropy' as loss, accuracy as metrics with batch size of 128 for 50 epochs. For CNN-LSTM model we used adam with learning rate of 10^{-4} and clipvalue of 1.0. We also used mean squared error as loss and RMSE as metrics and trained for 50 epochs with 128 batch size. 80% and 20% train-test split were used for all models.

3. Results and Discussion

This section presents the results of yoga pose classification and pose estimation using pressure-sensing matrix mat data, with comparisons to camera-based results. The section also discusses the classification accuracy, performance of the pose estimation, and custom real-world usage with continuous data flow (continuous dataset), which records the yoga poses continuously.

3.1 Yoga pose classification

Both the CNN (pressure data) and FCNN (camera data) models achieved high accuracy in classifying yoga poses, with F1-scores of 0.98 and 0.99, respectively, as in Table 1. The confusion matrices show that there are minimal misclassifications, indicating that pressure data alone is nearly as effective as camera data for pose recognition.

Table 1. Overall error metrics of FCNN and CNN models for yoga pose classification.

	FCNN			CNN		
	Precision	**Recall**	**F1-score**	**Precision**	**Recall**	**F1-score**
Macro Avg	0.99	0.99	0.99	0.99	0.98	0.98
Weighted Avg	0.99	0.99	0.99	0.98	0.98	0.98

3.2 Baseline model comparison

Baseline results of the models' accuracies are shown in Fig. 7. with random forest having the best accuracy with 91.47%, followed by CNN with 91.09%. However, when plotting out the confusion matrix, random forest, Fig. 15, is having difficulties differentiating "Free Style" poses where FCNN, Fig. 16, and CNN, Fig. 17, can well differentiate with FCNN correctly predicting 81 correct "Free Style" poses (See Figs. 15-17 in the Appendix).

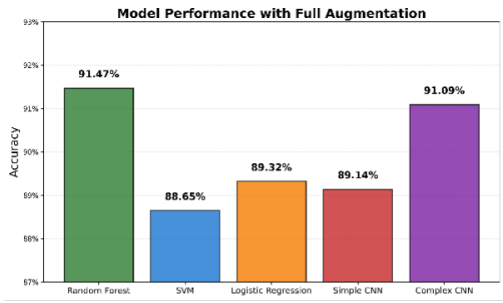

Fig. 7. Model accuracies for all models.

3.3 Pose estimation

The CNN-LSTM model was able to predict pose landmarks from pressure data sequences with an average root mean squared error (RMSE) of 0.062 using a 10-frame sequence (see Table 2). This demonstrates that pressure-based pose estimation is feasible, as it achieves accurate pose estimation without requiring vision-based input.

Table 2. Error metrics of pose estimation using CNN-LSTM.

Sequence Length (frames)	**5**	**10**	**20**	**30**
MSE	0.005	0.004	0.004	0.004
RMSE	0.071	0.062	0.063	0.062

3.4 Custom continuous flow data with less data

A custom continuous data recording protocol was implemented, capturing 10 seconds per pose with 5-second transitions

instead of discrete recordings. This approach better reflects real practice and provides richer data, even though we used significantly less data—about 500 samples per pose compared to the previous dataset, with over 5,000 average samples per pose. Despite the reduced dataset, training logs and performance plots Fig. 8 show that the model achieved high accuracy and adequate learning. The confusion matrix in Fig. 9 also confirms the robustness of the classification, with only minor confusion, as the "Free Style" pose occurs during pose transitions, when users must move from one position to another during pose changes. This continuous protocol improved both dataset realism and model generalization.

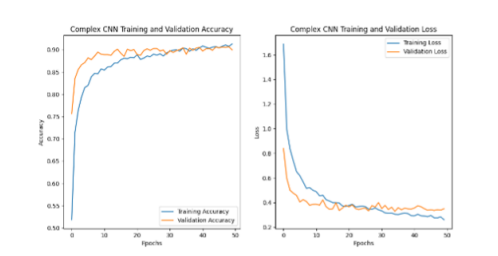

Fig. 8. Training and validation history for CNN model with continuous dataset; training and validation accuracy (left), and training and validation loss (right).

3.5 Usefulness and challenges

Compared with the vision-based systems, vision-based systems achieved OpenPose (99.58%) [5], CNN-LSTM (99.65%) [6], Yoga-82 dataset (up to 89.81%) [7], our system achieved (91.14%) while maintaining privacy.

Overall, a pressure-sensing matrix mat system for classifying yoga poses and pose estimation can compete with camera-based data when deep learning and appropriate preprocessing are used. Consistent with earlier studies on robust pose recognition using topological landmarks, this method provides a privacy-friendly and useful substitute for exercise monitoring [8]. However, as can be seen in Fig. 9, there are many false positives for the "Free Style" data because it occurs during the transitioning phase. Therefore, the real data may be the poses themselves. We can improve this result by removing the "Free Style" data, which is 1-2 seconds closer to the actual yoga pose. The usage of pose classification is illustrated in Fig. 10, while the extraction of pose estimation is demonstrated in Fig. 11.

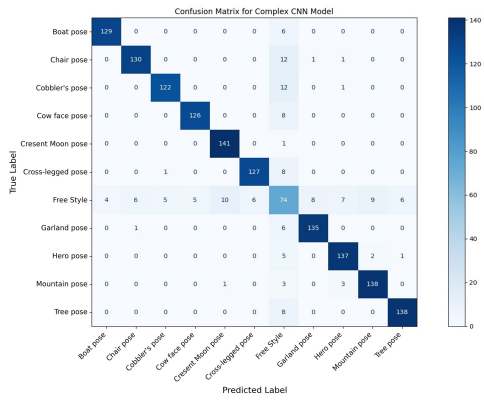

Fig. 9. Confusion matrix for CNN model with continuous dataset.

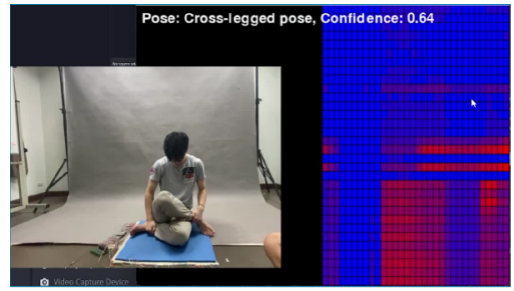

Fig. 10. Real-time yoga classification result.

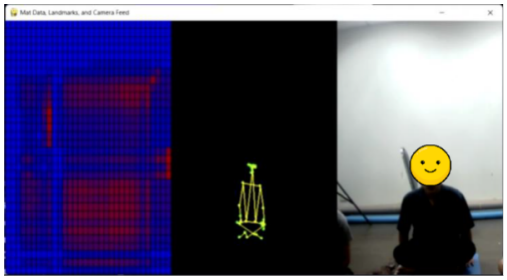

Fig. 11. Pose estimation result using pressure sensing matrix mat without reliance on the camera.

3.6 Comprehensive data augmentation impact analysis

As mentioned in Section 3.5, the models cannot predict "Free Style" well because many of the poses in the "Free Style" are the poses themselves. In this session, the models' accuracies were improved with the data cleaning by removing the "Free Style" data 2 seconds before and after the poses. As can be seen in Figs. 18-20, and Table 3 (see the Appendix), all models accuracies were improved from 3% to as much as 5%. This proves the hypothesis from Section 3.5.

3.7 Upper body errors and model size and latency

To quantify upper-body errors divide TP/FP, and the error percentages are shown below for 3 upper-body focus poses:

- Mountain pose: 6.8% error
- Tree pose: 1.4% error
- Crescent Moon: 15.5% error
- Average upper-body category: 6.5% error

Moreover, the model size and latency is also shown in Table A2 (see the Appendix).

4. Conclusion

We developed a pressure-sensing matrix mat system that uses a CNN model with 98% to classify yoga poses, which is closer to the 99% FCNN model used with camera data. We also did pose estimation from pressure data alone with the help of CNN-LSTM architecture. The classification models achieved high accuracy, and the pose estimation model produced a good RMSE of 0.062 with a 10-frame sequence, using only the pressure-sensing matrix mat. This demonstrates that the system can provide reliable, privacy-preserving pose analysis without the need for cameras. The results show strong potential for practical applications beyond yoga despite some limitations in upper body estimation and resource constraints. The potential for wider applications in physical rehabilitation, personalized fitness coaching, and healthcare monitoring is highlighted by the combination of deep learning and non-intrusive pressure sensors.

Acknowledgements

The first author (N.L.M.) acknowledges the Excellent Foreign Students (EFS) scholarship awarded by Sirindhorn International Institute of Technology, Thammasat University, Thailand, for his doctoral study..

References

[1] Posadzki P, Pieper D, Bajpai R, Makaruk H, Könsgen N, Neuhaus AL, Semwal M. Exercise/physical activity and health outcomes: an overview of Cochrane systematic reviews. BMC public health. 2020 Dec;20:1-2.

[2] Bull FC, Al-Ansari SS, Biddle S, Borodulin K, Buman MP, Cardon G, Carty C, Chaput JP, Chastin S, Chou R, Dempsey PC. World Health Organization 2020

guidelines on physical activity and sedentary behaviour. British journal of sports medicine. 2020 Dec 1;54(24):1451-62.

[3] Kramer A. An overview of the beneficial effects of exercise on health and performance. Physical Exercise for Human Health. 2020:3-22.

[4] Chithambaram N, Gupta A, Singh S, Nguyen TV. Virtual Yoga instructor with real-time feedback. In2025 59th Annual Conference on Information Sciences and Systems (CISS) 2025 Mar 19 (pp. 1-6). IEEE.

[5] Anand Thoutam V, Srivastava A, Badal T, Kumar Mishra V, Sinha GR, Sakalle A, Bhardwaj H, Raj M. Yoga pose estimation and feedback generation using deep learning. Computational Intelligence and Neuroscience. 2022;2022(1):4311350.

[6] Saurav S, Gidde P, Singh S. Exploration of deep learning architectures for real-time yoga pose recognition. Multimedia Tools and Applications. 2024 Oct;83(34):81621-63.

[7] Verma M, Kumawat S, Nakashima Y, Raman S. Yoga-82: a new dataset for fine-grained classification of human poses. In-Proceedings of the IEEE/CVF conference on computer vision and pattern recognition workshops 2020 (pp. 1038-1039).

[8] Mya NL, Deepaisarn S, Chonnaparamutt W, Laitrakun S, Nakayama M. Exercise Pose Recognition and Counting System using Robust Topological Landmarks. In 2023 18th International Joint Symposium on Artificial Intelligence and Natural Language Processing (iSAI-NLP) 2023 Nov 27 (pp. 1-6). IEEE.

[9] Fatema A, Chauhan S, Gupta MD, Hussain AM. Investigation of the long-term reliability of a velostat-based flexible pressure sensor array for 210 days. IEEE Transactions on Device and Materials Reliability. 2023 Dec 8;24(1):41-8.

[10] Clever HM, Erickson Z, Kapusta A, Turk G, Liu K, Kemp CC. Bodies at rest: 3d human pose and shape estimation from a pressure image using synthetic data. In-Proceedings of the IEEE/CVF conference on computer vision and pattern recognition 2020 (pp. 6215-6224).

[11] Casas L, Navab N, Demirci S. Patient 3D body pose estimation from pressure imaging. International journal of computer assisted radiology and surgery. 2019 Mar 14;14:517-24.

Appendix

Detailed model parameters in each layer for CNN, FCNN, and CNN-LSTM architectures are shown in Figs. 12-14, respectively. Figs. 15-17 shows the baseline confusion matrices for each model used for the pose classification. Performance improvements in data cleaning and augmentation are shown in Figs. 18-20, and the improvement percentage can also be seen in Table 3. Lastly, the size and latency of models used are described in Table 4.

Layer (type)	Output Shape	Param #
dense (Dense)	(None, 256)	34048
dropout (Dropout)	(None, 256)	0
dense_1 (Dense)	(None, 128)	32896
dropout_1 (Dropout)	(None, 128)	0
dense_2 (Dense)	(None, 64)	8256
dropout_2 (Dropout)	(None, 64)	0
dense_3 (Dense)	(None, 10)	650

Total params: 75,850
Trainable params: 75,850
Non-trainable params: 0

Fig. 12. FCNN model trained with estimated pose data from the camera.

Layer (type)	Output Shape	Param #
conv2d_12 (Conv2D)	(None, 32, 32, 32)	320
batch_normalization_16 (BatchNormalization)	(None, 32, 32, 32)	128
conv2d_13 (Conv2D)	(None, 32, 32, 32)	9248
batch_normalization_17 (BatchNormalization)	(None, 32, 32, 32)	128
max_pooling2d_6 (MaxPooling2D)	(None, 16, 16, 32)	0
dropout_10 (Dropout)	(None, 16, 16, 32)	0
conv2d_14 (Conv2D)	(None, 16, 16, 64)	18496
batch_normalization_18 (BatchNormalization)	(None, 16, 16, 64)	256
conv2d_15 (Conv2D)	(None, 16, 16, 64)	36928

...
Total params: 848,490
Trainable params: 846,826
Non-trainable params: 1,664

Fig. 13. CNN model architecture used for pressure sensing mat data.

Layer (type)	Output Shape	Param #
time_distributed_20 (TimeDistributed)	(None, None, 32, 32, 32)	320
time_distributed_21 (TimeDistributed)	(None, None, 32, 32, 32)	128
time_distributed_22 (TimeDistributed)	(None, None, 16, 16, 32)	0
time_distributed_23 (TimeDistributed)	(None, None, 16, 16, 64)	18496
time_distributed_24 (TimeDistributed)	(None, None, 16, 16, 64)	256
time_distributed_25 (TimeDistributed)	(None, None, 8, 8, 64)	0
time_distributed_26 (TimeDistributed)	(None, None, 8, 8, 128)	73856

...
Total params: 2,132,996
Trainable params: 2,130,500
Non-trainable params: 2,496

Fig. 14. CNN-LSTM architecture for pose estimation from the mat data.

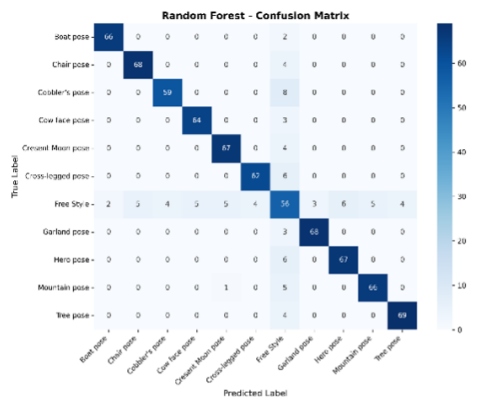

Fig. 15. Random forest confusion matrix.

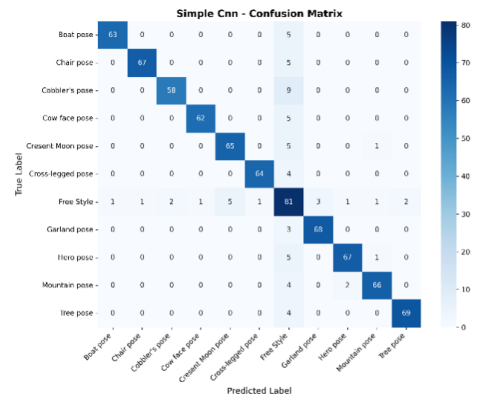

Fig. 16. FCNN confusion matrix.

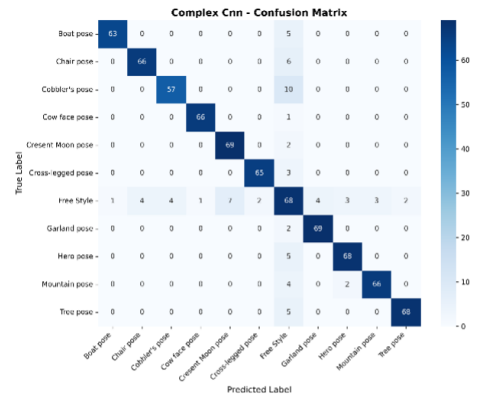

Fig. 17. CNN confusion matrix.

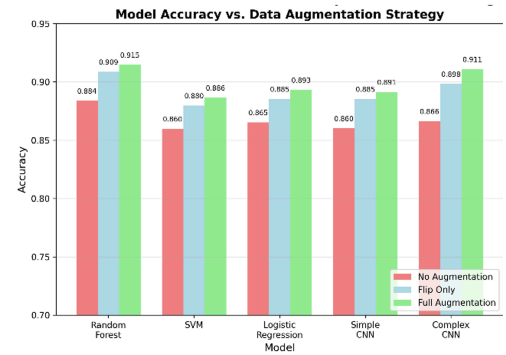

Fig. 18. Baseline accuracy vs. data augmentation accuracy.

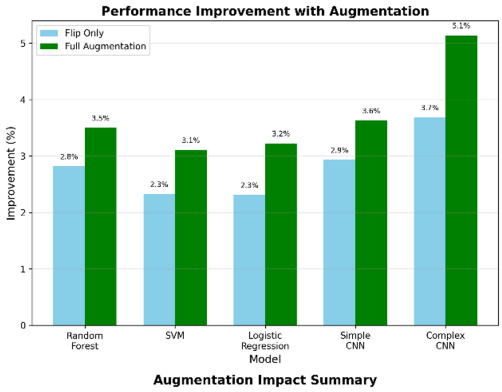

Fig. 19. Performance improvement with data augmentation.

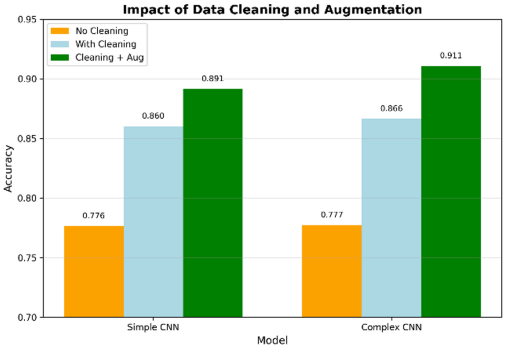

Fig. 20. Impact of data cleaning and augmentation.

Table 3. Improvement comparison from data augmentation.

Model	No Augmentation	Full Augmentation	Improvement
Random Forest	0.8838	0.9147	+3.5%
SVM	0.8598	0.8865	+3.1%
Logistic Regression	0.8653	0.8932	+3.2%
Simple CNN	0.8602	0.8914	+3.6%
Complex CNN	0.8664	0.9109	+5.1%

Table 4. Model size and latency.

Model	Size (MB)	Latency (ms)	Parameters
RF	13.58	0.044	N/A
SVM	17.14	0.621	N/A
LR	0.09	0.002	11,275
Simple CNN	3.65	0.678	315,275
Complex CNN	9.84	1.079	848,619